

**TAPE MECHANICS OVER A FLAT RECORDING HEAD UNDER UNIFORM PULL-DOWN
PRESSURE**

Sinan Müftü
Associate Professor
Department of Mechanical Engineering
Northeastern University, 334 SN
Boston, MA 02115-5000

Submitted in September 2002 and with revisions December 2002

Accepted for publication in:
Microsystem Technologies
Micro-and Nanosystems. Information Storage and Processing Systems

Abstract

The mechanics of the "tape" over a flat-head is investigated. It has been recently shown that a thin, flexible tape, traveling over a flat recording head under tension contacts the head over the central area of the head. This phenomenon is due to the *self-acting, subambient foil bearing effect*. In this paper, as a first order of approximation, a simplified system is analyzed; where a *uniform* subambient pressure p^* is assumed to be acting on the tape, over the head region. Increasing subambient pressure values represent faster tape speeds. This approach enables an independent investigation of the tape mechanics alone, and provides a closed-form solution. The tape is modeled as a tensioned infinitely wide plate, travelling at steady state. This non-dimensional solution relates the tape displacements and the reaction forces to the problem parameters, i.e., the wrap angle, tape tension, bending rigidity, head-length and external pressure. Tape and head-wear at the corners of the head, and wear of the magnetically active regions located at the central part of the flat-head are critical issues to be considered in designing a flat-head/tape interface. The closed-form solution is particularly useful in obtaining estimates of the magnitudes of the reaction forces at the corners.

Nomenclature

| | | | |
|----------------|--|--------------|--|
| w^* | Tape displacement | w | $= w^* / c$ |
| x^* | Coordinate axis | x | $= x^* / L_H$ |
| p^* | Magnitude of uniform pressure | p | $= 12(1-\mathbf{u}^2)(p^* / E)(L_H / c)^4$ |
| L_H | Head length | \mathbf{q} | $= \mathbf{q}^* L_H / c$ |
| D | Bending rigidity $D = Ec^3/12(1-\mathbf{n}^2)$ | Δ | $= L_H / b$ |
| T | Tension per unit width | b | $= \sqrt{D/T_{eff}}$ |
| T_{eff} | Effective tension, $T-\mathbf{r}V^2$ | F_0 | $= F_0^* L_H^3 / Dc$ |
| V | Tape speed | F_L | $= F_L^* L_H^3 / Dc$ |
| E | Elastic modulus | U | $= U^* L_H / T_{eff} c^2$ |
| c | Thickness | | |
| \mathbf{n} | Poisson's ratio | | |
| \mathbf{r} | Tape mass per area | | |
| H | Heaviside function | | |
| \mathbf{q}^* | Wrap angle | | |
| F_0^* | Edge reaction force/width | | |
| F_L^* | Inner contact reaction force/width | | |
| U^* | Strain energy density | | |

Introduction

The *foil bearing problem* describes the self-acting lubrication phenomenon between a thin, flexible tape moving over a *cylindrical* surface under tension. Such applications are found over magnetic tape recording heads, and rollers in various web handling applications. The deflections of the tape and super-ambient air pressure that forms in the head/tape interface, due to the self-acting air bearing, are strongly coupled. The mechanics and solution of the foil bearing problem have been reported by many investigators, including the following references [1-7]. In order to minimize the signal loss, modern tape recording applications require the tape to be in contact with the recording head, during the read/write operations. However, keeping the tape in contact with the head is a challenging task with cylindrically contoured heads, in which the mostly superambient air pressure in the head-tape interface, caused by the self-acting air bearing, tends to separate the tape from the head.

It has been shown that when a *flat* recording head is used instead of a cylindrical one, reliable contact is obtained over the central region of the flat-head [8-13]. This recent finding has sparked interest in the mechanics and tribology of such systems. Flat-heads have been recently implemented in commercial tape recorders. There are several technical and commercial advantages to using flat-heads. In particular, faster tape speeds over flat-heads have been shown to provide more reliable contact, in direct contrast to tape behavior over cylindrical heads. Moreover, the flat contour is more forgiving for tapes with different thickness, enabling backward/forward compatibility of tapes. Finally, flat-heads are considerably easier to manufacture as compared to contoured heads. Tape and head-wear at the corners of the head, and wear of the magnetically active regions located at the central part of the flat-head are critical issues to be considered in designing a flat-head/tape interface. We address this issue among others in this paper.

The mechanics of a tensioned tape moving over a flat-head is interesting. One explanation of this operation involves the assumption that the sharp leading edge of the recording head removes air from the surface of the magnetic medium, creating a vacuum under the tape; Then the pressure differential between the top and the bottom surfaces of the tape push it down toward the recording head surface [8,9]. A considerably more complete model of the head-tape interface, including the effects of a) the mechanics of a translating tape, b) air lubrication using Reynolds equation, and c) surface roughness, showed that the contact is provided due to the *self-acting, subambient foil bearing* effect [10-12]. The analysis showed that air entrained in the flat-head/tape interface forms a subambient pressure layer, because the tape wrapped over a flat surface creates a diverging channel at the leading edge. The subambient air pressure over the flat-head region eventually pulls the tape down to contact the head. The mechanics of the tape and air lubrication are strongly coupled in the *subambient foil bearing*.

In the case of cylindrical heads, contact can be obtained by increasing the tape tension. In contrast, in the case of flat-heads, the subambient air bearing causes the desired contact. Thus the mechanics of the flat-head/tape interface is fundamentally different from that of the cylindrically contoured one.

Müftü and Kaiser used a commercially available two-wavelength interferometer, to measure the head/tape spacing for a wide range of parameters [13]. Comparison of the measurements to the model results was very good. This work confirmed that the tape forms two displacement bumps near the leading and trailing edges of the flat-head, and

these bumps are, in general, connected with a flat region where the tape contacts the head. It was shown that the length of the displacement bumps is the critical dependent variable, which increases at higher wrap angle and tape tension values; and decreases with increasing tape speed [13].

In this paper the mechanics of the tape deformation underlying the operation of a flat-head/tape interface is investigated analytically. As a first order of approximation, a simplified system is analyzed, where a uniform subambient pressure p^* is assumed to be acting on the tape, only over the head region. Note that increasing subambient pressure p^* , in general, can be thought to represent faster tape speed¹. Figure 1 shows the generic geometry that is considered. The problem is modeled with a constant coefficient, ordinary differential equation, and a closed-form solution is given in normalized coordinates. It is found that the tape mechanics for this problem needs to be analyzed in three *cases* for no-contact, point-contact and area-contact on the central part of the head, named later in the paper case-1, -2 and -3, respectively. Therefore, three different solutions are found for each case. The critical pressure values causing the transition between these cases are identified. Among others, it should be underlined that the solution provided here is particularly useful in obtaining the magnitudes of the reaction forces at the corners of the flat-head. In this work, the corners of the head are assumed to be unworn, hence the concentrated reaction forces develop on the corners. In practice, the corners will be beveled and the corner reaction will be distributed over an area.

The Governing Equation

Tape is modeled as an infinitely wide tensioned plate, travelling at steady state,

$$D \frac{d^4 w^*}{dx^{*4}} - (T - \mathbf{r}V^2) \frac{d^2 w^*}{dx^{*2}} = -p^* (H(x^*) - H(x^* - L_H)). \quad (1)$$

The variables of this equation are defined in the nomenclature. The Heaviside function is defined such that $H(x^*) = 1$ when $x^* \geq 1$ and zero, otherwise. Note that the first term on the left-hand side of this equation represents the bending stiffness, and the second term represents the in-plane tension effects. The $\mathbf{r}V^2 d^2 w^* / dx^{*2}$ term represents the centrifugal acceleration, which is the only remaining term of total acceleration at steady state [5]. A schematic of the modeled system is given in Figure 1; a uniform downward pressure p^* acts on the tape over the head region, $0 \leq x^* \leq L_H$; the tape is wrapped symmetrically around the head with wrap angles \mathbf{q}^* . The following non-dimensional variables are introduced,

$$x = \frac{x^*}{L_H}, \quad w = \frac{w^*}{c}, \quad p = 12(1 - \mathbf{n}^2) \frac{p^*}{E^*} \left(\frac{L_H}{c} \right)^4, \quad \mathbf{q} = \frac{L_H \mathbf{q}^*}{c}, \quad \Delta = \frac{L_H}{b}, \quad b = \left(\frac{D}{T_{eff}} \right)^{1/2} \quad (2)$$

where the effective tension is defined as $T_{eff} = T - \mathbf{r}V^2$. Then equation (1) becomes,

¹ Numerical analysis from reference [12] shows that the (gauge) pressure values of 0, -12.1, -32.4 and -39.4 kPa are obtained under the flat part of the tape, for tape transport speeds of 0.8, 1.6, 4, and 8 m/s, respectively. The other parameters of this problem were $L_H = 1.5$ mm, $c = 15 \mu\text{m}$, $E = 4$ GPa, $\mathbf{q}^* = 1.5^\circ$, $T = 43$ N/m [12].

$$\frac{d^4 w}{dx^4} - \Delta^2 \frac{d^2 w}{dx^2} = -p(H(x) - H(x-1)), \quad (3)$$

where b is the *characteristic bending length*. The non-dimensional head length Δ can also be expressed as follows,

$$\Delta = 2\sqrt{3(1-n^2)} \frac{L_H T_{eff}^{1/2}}{E^{1/2} c^{3/2}}. \quad (4)$$

Thus when all other parameters are constant, increasing Δ values can be interpreted as increasing the effective tape tension T_{eff} . Note that in this analysis p , Δ and q are the independent parameters of the analysis.

As the tape is wrapped symmetrically under tension around a flat surface with wrap angle q , it initially takes a cupped shape; and reaction forces F_0 develop at the edges of the flat surface, as shown in Figure 2a. Then, as a uniform subambient pressure p is applied on the tape, over the head region, the tape starts to deform downward, toward the head surface. The deformation behavior of the tape under these conditions can be analyzed in three *cases* as depicted in Figure 2. The explanation of these cases and the related boundary conditions are given next. Note that in this paper "increasing pressure" implies increasing subambient pressure.

- Case-1: Typically, as p increases from zero, the tape will deflect toward the surface of the head; eventually, when the pressure reaches a critical value, $p = p_{cr}^{(1)}$, the tape will just touch the head at $x = 1/2$. At this level of pressure p no reaction force develops between the tape and the central portion of the head. The tape behavior when $0 < p \leq p_{cr}^{(1)}$ constitutes *case-1*.
- Case-2: When the pressure level is increased above the first critical pressure, $p > p_{cr}^{(1)}$ a reaction force, F_L , develops between the tape and the head; and the tape continues to deform with a single contact point at $x = 1/2$. Eventually, when the pressure magnitude equals a second critical value, $p = p_{cr}^{(2)}$, the curvature of the tape at the contact point becomes zero. During this process the reaction force in the center keeps increasing while the tape contacts the head only at $x = 1/2$. The tape behavior when $p_{cr}^{(1)} < p \leq p_{cr}^{(2)}$ constitutes *case-2*.
- Case-3: If the external pressure is increased even further, $p > p_{cr}^{(2)}$, then the contact point moves closer to the edges of the head; the tape contacts the head in the region, $L \leq x \leq 1-L$, where $L < 1/2$. In this "flat" region $w = 0$. While $p > p_{cr}^{(2)}$ two distinct displacement bumps form near the edges of the head, in $0 \leq x \leq L$ and $1-L \leq x \leq L$. In the flat region, the value of the contact pressure between the head and the tape is equal to the external pressure p . At the edges of the flat region reaction forces F_L develop. The tape behavior when $p > p_{cr}^{(2)}$ constitutes *case-3*.

The tape deformation for the three contact cases described above are obtained by solving equation (3). Here this equation is solved in a piecewise manner for each one of the cases,

$$w = \begin{cases} w^{(1)} & \text{for } x \leq 0 \\ w^{(2)} & \text{for } 0 \leq x \leq 1, \\ w^{(3)} & \text{for } x \geq 1 \end{cases} \quad (5)$$

where $w^{(i)}$ ($i = 1, 2, 3$) are the tape deflections to the left of the head, over the head and to the right of the head, respectively, as shown in Figure 1. The tape supports are assumed to be found as $x \rightarrow \pm\infty$. Note that for each case described above, a different $w^{(i)}$ expression will be found.

For all three cases, in regions away from the head, the slope of the tape approaches the wrap angle and the tape displacements must remain bounded. Thus the boundary conditions on the left and right sides of the tape become,

$$\begin{aligned} x \rightarrow -\infty: \quad w_{,x}^{(1)} = \mathbf{q}, \text{ (a) and } w^{(1)} \text{ is bounded (b)} \\ x \rightarrow \infty: \quad w_{,x}^{(3)} = -\mathbf{q}, \text{ (c) and } w^{(3)} \text{ is bounded (d)} \end{aligned} \quad (6)$$

where the subscripted comma indicates differentiation.

On the edges of the head, $x = 0$ and $x = 1$, the tape displacement, slope and curvature need to be continuous. These conditions apply for all three cases described above, and they are represented by the following boundary conditions,

$$\begin{aligned} x = 0: \quad w^{(1)} = w^{(2)} = 0 \text{ (a,b), } w_{,x}^{(1)} = w_{,x}^{(2)} \text{ (c), } w_{,xx}^{(1)} = w_{,xx}^{(2)} \text{ (d)} \\ x = 1: \quad w^{(2)} = w^{(3)} = 0 \text{ (e,f), } w_{,x}^{(2)} = w_{,x}^{(3)} \text{ (g), } w_{,xx}^{(2)} = w_{,xx}^{(3)} \text{ (h)} \end{aligned} \quad (7)$$

In case-3, the tape displacement, slope and curvature are zero at the inner contact point $x = L$, shown in Figure 2c,

$$x = L \text{ and } 1 - L: \quad w^{(2)} = 0 \text{ (a), } w_{,x}^{(2)} = 0 \text{ (b), } w_{,xx}^{(2)} = 0 \text{ (c)}. \quad (8)$$

In contrast, in case-2, the tape displacement and slope are zero at the center of the head $x = 1/2$, but the curvature is non zero; hence, only equations (8a,b) apply.

Note that the mechanics of the displacement bumps that form on the left and the right sides of the head, in case-3, do not affect each other. Therefore, only solution of the bump on the left will be given here. The results for the second bump can be obtained by letting $x \rightarrow 1 - x$ once the solution is found.

Solutions

Case-1

The tape displacement for case-1 is obtained by solving equation (3) with the boundary conditions (6) and (7). Thus the following piecewise solution is obtained:

$$w(x) = \begin{cases} \mathbf{q}x - \frac{1}{4\Delta} \left[\frac{p}{\Delta^2} \left(\left(1 - \frac{2}{\Delta}\right) + \left(1 + \frac{2}{\Delta}\right)e^{-\Delta} \right) + 2(1 + e^{-\Delta})\mathbf{q} \right] (e^{\Delta x} - 1), & \text{for } x \leq 0 \\ \frac{1}{2} \frac{p}{\Delta^2} (x^2 - x) - \frac{1}{4\Delta} \left[\frac{p}{\Delta^2} \left(1 + \frac{2}{\Delta}\right) + 2\mathbf{q} \right] \left[(e^{-\Delta x} - 1) + (e^{\Delta(x-1)} - e^{-\Delta}) \right], & \text{for } 0 \leq x \leq 1 \\ \mathbf{q}(1-x) - \frac{1}{4\Delta} \left[\frac{p}{\Delta^2} \left(\left(1 - \frac{2}{\Delta}\right) + \left(1 + \frac{2}{\Delta}\right)e^{-\Delta} \right) + 2(1 + e^{-\Delta})\mathbf{q} \right] (e^{\Delta(1-x)} - 1), & \text{for } x \geq 1 \end{cases} \quad (9)$$

The first critical pressure $p_{cr}^{(1)}$, where the mid-point deflection becomes zero, can be obtained by setting $w(1/2) = 0$, which results in,

$$p_{cr}^{(1)} = \frac{4\mathbf{q}\Delta (e^{-\Delta/2} - 1)^2}{1 - \frac{2}{\Delta} \left(1 + \frac{2}{\Delta}\right) (e^{-\Delta/2} - 1)^2}. \quad (10)$$

The critical pressure $p_{cr}^{(1)}$ varies linearly with the wrap angle \mathbf{q} , but a non-linear relation exists between the parameter Δ and $p_{cr}^{(1)}$.

Case-3

Case-2 is a limiting case of case-3, therefore, the solution of case-3 is presented first. The tape displacement for case-3 is obtained by solving equation (3) with the boundary conditions (6) and (7a-d) and (8a,b). This gives the following piecewise solution,

$$w(x) = \begin{cases} \mathbf{q}x + \left(\mathbf{a}_1 + \mathbf{a}_2 + \frac{p}{\Delta^4} \right) (e^{\Delta x} - 1), & \text{for } x \leq 0 \\ -(\mathbf{a}_1 + \mathbf{a}_2) + \left(\mathbf{q} + 2\Delta\mathbf{a}_1 + \frac{p}{\Delta^3} \right) x + \mathbf{a}_1 e^{-\Delta x} + \mathbf{a}_2 e^{\Delta x} + \frac{px^2}{2\Delta^2}, & \text{for } 0 \leq x \leq L \end{cases} \quad (11)$$

where the coefficients \mathbf{a}_1 and \mathbf{a}_2 are,

$$\mathbf{a}_1 = - \frac{e^{\Delta L} \left\{ \left[2 + 2\Delta L + ((\Delta L)^2 - 2) e^{\Delta L} \right] \frac{p}{\Delta^2} + 2\Delta \left[1 + (\Delta L - 1) e^{\Delta L} \right] \mathbf{q} \right\}}{2\Delta^2 \left\{ -1 + 4e^{\Delta L} + [2\Delta - 3] e^{2\Delta L} \right\}} \quad (12a)$$

$$\mathbf{a}_2 = \frac{\left\{ - \left[2 + \Delta L (4 + \Delta L) + 2(\Delta L (\Delta L - 1) - 1) e^{\Delta L} \right] \frac{p}{\Delta^2} + 2\Delta \left[e^{\Delta L} - 1 - \Delta L \right] \mathbf{q} \right\}}{2\Delta^2 \left\{ -1 + 4e^{\Delta L} + [2\Delta - 3] e^{2\Delta L} \right\}} \quad (12b)$$

Equation (11) shows that the tape displacement is a linear function of tape wrap angle \mathbf{q} , and external pressure p ; and that it depends on the non-dimensional head length Δ in a

nonlinear fashion. Equation (11) is valid for specific pairs of L and p values: The relation between the bump length L and the external pressure p is established from the last boundary condition, equation (8c), $d^2w/dx^2(L) = 0$, which results in,

$$p = \frac{\Delta^3 (e^{2\Delta L} (1 - 2\Delta L) - 1) \mathbf{q}}{2(e^{\Delta L} - 1)^2 + \Delta(1 + 2e^{\Delta L} - 3e^{2\Delta L}) + \Delta^2 L^2 e^{\Delta L} (1 + e^{\Delta L})}. \quad (13)$$

Case-2

The tape displacement for case-2 can be obtained from equation (11) for p values in the range $p_{cr}^{(1)} < p \leq p_{cr}^{(2)}$; and by letting $L = 1/2$. This affects the constants \mathbf{a}_1 and \mathbf{a}_2 ; whose modified forms will not be given here in order to save space. The second critical pressure $p_{cr}^{(2)}$ is obtained from equation (13) by letting $L = 1/2$, which gives,

$$p_{cr}^{(2)} = \frac{\Delta^3 (e^\Delta (1 - \Delta) - 1) \mathbf{q}}{2(e^{\Delta/2} - 1)^2 + \Delta(1 + 2e^{\Delta/2} - 3e^\Delta) + \frac{\Delta^2}{4} e^{\Delta/2} (1 + e^{\Delta/2})}. \quad (14)$$

Reaction forces

Contact between the tape and the flat-head gives rise to concentrated reaction forces F_0 and F_L at $x = 0$, and at $x = L$, respectively; and a region of uniform contact pressure in $L < x < 1 - L$, as depicted in Figure 2. An understanding of the magnitude of the reaction forces and the contact pressure is especially important in flat-head design because head and tape wear are closely related to these variables. The reaction forces F_0 and F_L are obtained from the following relations,

$$F_0 = \left[\frac{d^3 w^{(2)}}{dx^3} - \frac{d^3 w^{(1)}}{dx^3} \right]_{x=0} \quad (\text{a}) \quad \text{and} \quad F_L = \left[-\frac{d^3 w^{(2)}}{dx^3} \right]_{x=L} \quad (\text{b}). \quad (15)$$

Note that the non-dimensional reaction forces are defined as $F_0 = F_0^* L_H^3 / Dc$ and $F_L = F_L^* L_H^3 / Dc$, where F_0^* and F_L^* are the reaction forces per unit width.

Reaction force at the edge

Using equation (9) in (15a), the reaction force F_0 at the edge of the head for case-1 becomes,

$$F_0 = \frac{1}{2} (p + 2\Delta^2 \mathbf{q}) \quad \text{for} \quad 0 \leq p \leq p_{cr}^{(1)}. \quad (16)$$

Note that this expression can also be obtained by considering the force equilibrium in the vertical direction.

In order to find the reaction force F_0 for case-2, equation (15a) is evaluated with equation (11) by letting $L = 1/2$. This results in the following expression,

$$F_0 = \frac{\Delta}{4e^{\Delta/2} - 1 + e^{\Delta}(2\Delta - 3)} \left\{ \left[1 + 2e^{\Delta/2} \left(\frac{\Delta}{2} - 1 \right) + e^{\Delta} \left(1 - 2\Delta - \frac{\Delta^2}{4} \right) \right] \frac{p}{\Delta^2} + 2e^{\Delta/2} \Delta \left[1 + e^{\Delta/2} \left(\frac{\Delta}{2} - 1 \right) \right] \mathbf{q} \right\} . \quad (17)$$

for $p_{cr}^{(1)} < p \leq p_{cr}^{(2)}$

The reaction force F_0 at the edge of the head for case-3 is found from equations (11) and (15) as follows,

$$F_0 = \frac{\Delta}{4e^{\Delta L} - 1 + e^{2\Delta L}(2\Delta - 3)} \left\{ \left[1 + 2e^{\Delta L}(\Delta L - 1) + e^{2\Delta L}(1 - 2\Delta - \Delta^2 L^2) \right] \frac{p}{\Delta^2} + 2e^{\Delta L} \Delta \left[1 + e^{\Delta L}(\Delta L - 1) \right] \mathbf{q} \right\} \text{ for } p > p_{cr}^{(2)} . \quad (18)$$

Note that in evaluating F_0 for case-3, equation (18) should be used together with equation (13), in order to obtain the proper L and p values.

Reaction force at $x = L$

Contact between the tape and the head occurs on the central part of the flat-head when $p \geq p_{cr}^{(1)}$. For case-2, when the magnitude of the uniform pressure is in the range $p_{cr}^{(1)} < p \leq p_{cr}^{(2)}$ contact occurs only at the center ($x = 1/2$) of the head, and the resulting concentrated reaction force F_L can be calculated by using equations (15b) and (11) with $L = 1/2$. This gives the reaction force at $x = 1/2$ for case-2,

$$F_L = -\Delta^3 \left[-\mathbf{a}_1 e^{-\Delta/2} + \mathbf{a}_2 e^{\Delta/2} \right] \quad (19)$$

where \mathbf{a}_1 and \mathbf{a}_2 are given by equation (12) with setting $L = 1/2$.

In case-3, where the magnitude of the external pressure is greater than $p_{cr}^{(2)}$, the tape contacts the head in the central region $L \leq x \leq 1 - L$. At the edges of this region, $x = L, 1 - L$, the reaction force between the tape and the head is obtained from equations (15b) and (11). Thus the reaction force at $x = L$ for case-3 becomes,

$$F_L = -\Delta^3 \left[-\mathbf{a}_1 e^{-\Delta L} + \mathbf{a}_2 e^{\Delta L} \right]. \quad (20)$$

Note that equation (13) should be used along with the above relation in order to determine the proper relation between p and L . Finally, inside the contact region $L < x < 1 - L$ the contact pressure is equal to p .

Discussion of the Results

Typical values of the parameters of a tape recording application are given in Table 1, in both dimensional and non-dimensional forms. This table shows that pull down pressure values to be in $0 < p < 5,000$ range. It was mentioned in the Introduction that increasing values of p^* indicate increasing tape speed. The p value is equal to 10,750 for the example taken from reference [12]. In the following, the results are presented for a large range of pressures ($1 < p < 10^5$) in order to account for combination of the physical parameters that are different than those given in Table 1.

Tape displacement behavior

The mid-point displacement of the tape w_m , in case-1, before the tape contacts the head in the center is obtained from equation (9) as follows,

$$w_m = w^{(2)}\left(\frac{1}{2}\right) = \frac{1}{4} \left[\left(\frac{1}{\Delta} + \frac{2}{\Delta^2} \right) \left(e^{-\Delta/2} - 1 \right)^2 - \frac{1}{2} \right] \frac{p}{\Delta^2} + \frac{1}{2\Delta} \left(e^{-\Delta/2} - 1 \right)^2 \mathbf{q}. \quad (21)$$

This equation shows that w_m varies linearly with the external pressure p and the wrap angle \mathbf{q} . Its relation to the parameter Δ is non-linear. The variation of w_m as a function of Δ , for $p = 0$ and 50 and $\mathbf{q} = 3, 6$ and 9 is plotted in Figure 3. This plot shows that for a given pressure p a unique value of Δ exists for contact to take place; when $p = 0$, contact occurs as $\Delta \rightarrow 0$; and, when $p = 50$, contact occurs at higher Δ values depending on the wrap angle \mathbf{q} . Increasing Δ causes the tape displacement to increase until a critical value Δ_{cr} is reached, after which w_m decreases. This indicates that, initially, increasing Δ causes the tape to become more "cupped" over the head; but as Δ becomes greater than Δ_{cr} the tape "flattens."

The effect of this interesting result, on the overall tape displacement is shown in Figure 4 for $p = 50$ and $\mathbf{q} = 6$. Part a) of this figure shows the case of $\Delta < \Delta_{cr}$, and part b) shows the case of $\Delta > \Delta_{cr}$, where the "cupping" and "flattening" effects are observed, respectively. The strain energy density calculations given in the appendix show that as $\Delta \rightarrow 0$ the tape deformation is dominated by bending stiffness; as $\Delta \rightarrow \Delta_{cr}$ the effect of bending stiffness on the deformation is reduced, and the tension stiffness of the tape peaks at $\Delta = \Delta_{cr}$; finally, as $\Delta > \Delta_{cr}$ the bending and tension stiffness become close to each other. Thus it is seen that the occurrence of the displacement peak in Figure 3 is related to maximum tension stiffness of the tape.

The critical value of the parameter Δ is obtained by setting $w_{m,\Delta} = 0$, which results in the following non-linear equation,

$$\frac{-8 - (3 + \Delta_{cr})\Delta_{cr} + (4 + \Delta_{cr})^2 e^{-\Delta_{cr}/2} - (8 + 5\Delta + \Delta^2) e^{-\Delta}}{2e^{-\Delta_{cr}} \left(e^{\Delta_{cr}/2} - 1 \right) \left(1 + \Delta_{cr} - e^{\Delta_{cr}/2} \right) \Delta_{cr}^3} - \frac{\mathbf{q}}{p} = 0 \quad (22)$$

The solution of this equation is plotted in Figure 3 along with the mid-point displacement w_m given in equation (15). It is interesting to note that the smallest value of Δ_{cr} ($=2.51$) occurs when $p = 0$. In other words, when there is no external loading on the tape, the change in displacement behavior of the tape occurs when $\Delta_{cr} = 2.51$; and this value is independent of the wrap angle \mathbf{q} . In contrast, when there is external load acting downward on the tape, the critical value of the parameter Δ occurs after 2.51; and in this case the critical value depends on the wrap angle.

In case-3, where $p > p_{cr}^{(2)}$, the tape contacts the head, and two displacement "bumps" appear symmetrically near the edges. The displacement bump on the left spans the range $0 \leq x \leq L$, where $L < 1/2$. Both of the bumps are depicted schematically in Figure 2. Figure 5 shows the tape displacements under different loads p for $\Delta = 10$ and 50, and $\theta = 6$. In Figure 5a, where $\Delta = 10$ the critical loads are $p_{cr}^{(1)} = 310$ and $p_{cr}^{(2)} = 458$,

the displacements are plotted for the left half of the tape for p values in the range 0 – 2542. For case-1, ($p = 0, 155$) increase in the load results decrease in tape displacement, but no contact occurs as predicted. For case-2, where the load is in the range $p_{cr}^{(1)} < p \leq p_{cr}^{(2)}$ the tape contacts at the center of the head, and deforms slightly downward as the load is increased from $p_{cr}^{(1)}$ to $p_{cr}^{(2)}$. For case-3, ($p = 944, 2542$) increasing p causes the displacement bump height and the length to become smaller.

Figure 5b shows a similar analysis for $\Delta = 50$, where the critical loads are $p_{cr}^{(1)} = 1252$ and $p_{cr}^{(2)} = 1359$. Displacement behavior in this case is similar to the one presented in Figure 5a. Figures 5a and 5b are plotted for the same contact lengths, $L = 0.33$ and 0.25 . Close inspection of the loads shows that for a given L value, contact occurs at a higher p when Δ is increased; For example, for $L = 0.33$ contact occurs at $p = 944$ and 2523 for $\Delta = 10$ and 50 , respectively. This is an other indication of tape becoming stiffer at higher Δ values.

Length of the displacement bump, L , in case-3

The relation between L and p for case-3, given by equation (13), is plotted on log-log scale in Figure 6a for $\Delta = 1$ and 50 and $q = 3, 6$ and 9 . A nearly linear relation between L and p on the log-log scale exists. Note that, on the low end of the p -axis, this figure confirms that p is limited by $p_{cr}^{(2)}$ and that L is limited by $1/2$. As p increases the bump length L takes smaller values. This figure also shows that for a given load p , a) the bump length increases with increasing the wrap angle; and, b) the bump length increases with increasing Δ value.

Figure 6b shows the peak height of the displacement bump, $w(L_p)$, for case-3 as a function of the external load p . The corresponding location $x = L_p$ is obtained by setting $w_{,x}^{(2)} = 0$ in equation (11); this results in a non-linear relation, from which L_p is found numerically. Figure 6b shows that as pressure increases the peak height of the bump decreases. For $\Delta = 1$ this dependence is linear on the log-log scale, and for $\Delta = 50$ the peak height is nearly independent of p . Similar to L - p relation curve, above, the peak height curve is also limited by $p_{cr}^{(2)}$ on the lower p -range.

Reaction forces

Finally, the variation of the reaction forces F_0 and F_L as a function of the external load p for $\Delta = 10$, and 50 and $q = 3, 6$ and 9 are plotted in Figure 7. This figure is plotted for all three cases described above, using equations (16)-(18) for F_0 and equations (19) and (20) for F_L . The $p_{cr}^{(2)}$ value can be easily observed in these plots where F_L drops precipitously. Plots 7a and 7b clearly show that as p approaches zero, the edge reaction force approaches $F_0 \rightarrow q\Delta^2$ ($F_0^* \rightarrow q^* T_{eff}^*$); however, this effect occurs when there is no contact in the center ($p < p_{cr}^{(2)}$). The external pressure p starts to affect the reaction force on the edge F_0 , when the tape starts contacting in the center ($p > p_{cr}^{(2)}$); this effect becomes more pronounced at lower Δ values. For high p values the external force

dominates the magnitudes of both of the reaction forces, F_0 and F_L . The magnitude of the reaction force F_L at edge of the central contact area is, in general, lower than the edge force F_0 . The difference between the two reaction force becomes more pronounced at low p -range and for high Δ values.

Summary and Conclusions

The mechanics of the tape underlying the operation of a flat-head/tape interface is investigated with a uniform subambient pressure p acting on the tape over the head region. A closed-form solution is obtained in non-dimensional form. This solution is used to relate the tape displacements and the reaction forces to the problem parameters, i.e., the wrap angle, tape tension, bending rigidity, head-length and external pressure. The solution shows that as the magnitude of the uniform subambient pressure is increased, three different cases of contact behavior exist for the central region of the head; no contact (case-1), point contact (case-2) and area-contact (case-3). The critical pressure values causing the transition between these cases are found.

In case-1, a critical non-dimensional head width Δ_{cr} was found; for fixed p and q , increasing Δ while $\Delta < \Delta_{cr}$ causes the peak tape displacement to increase; and increasing Δ beyond Δ_{cr} causes the peak displacement to decrease. This behavior is associated with peaking of the tension stiffness of the tape near $\Delta = \Delta_{cr}$.

Expressions for the reaction forces on the edges of the head F_0 , and the edges of the inner contact region F_L are found. For a given external load p , F_0 is considerably higher than F_L ; and, the difference grows with increasing Δ . For low p values, the reaction force at the edge of the head F_0 approaches the normal component of the external tension ($q^* T_{eff}$); for large p values, F_0 is dominated by p .

The solution provided here is useful to identify the effects of *some* of the operating parameters of the full self-acting subambient foil bearing problem, where the Reynolds equation and asperity contact are involved. In the future, the results of the current work will be compared with the results of a numerical solution, including the effects of the bearing number and asperity compliance.

References

1. Eshel, A. and Elrod, H.G., "Theory of infinitely wide, perfectly flexible, self acting foil bearing," *J. Basic Engineering*, 1965, Dec., pp. 831-836.
2. Gross W.A. Fluid Film Lubrication. *John Wiley & Sons, NY 1980*.
3. Stahl, K.J., White, J.W. and Deckert, K.L., "Dynamic response of self acting foil bearings," *IBM Journal of Research and Development*, 1974, pp. 513-520.
4. Lacey C. and Talke F. Measurement and simulation of partial contact at the head/tape interface. *Journal of Tribology* 1992, 144, 646-652.
5. Müftü S. and R.C. Benson, "A Study on Width-Wise Variations in the Two Dimensional Foil Bearing Problem", *Journal of Tribology, Trans. ASME*, 1996, Vol. 118, No.2, pp. 407-414.
6. Lakshmikumar, A. and Wickert, J.A., "Equilibrium analysis of finite width tension dominated foil bearings," *Journal of Tribology, Trans ASME*, 1998, 121, pp. 108-113.
7. Ducotey, K. S. and Good, J. K., "A numerical algorithm for determining the traction between a web and a circumferentially grooved roller," *Journal of Tribology, Trans ASME*, 2000, 122, pp. 578-584.
8. DeMoss D.L. Flat Magnetic Heads. *US Patent No. US3737582, 1973*.
9. Biskeborn R.G and Eaton J.H., Bidirectional flat contour linear tape recording head and drive. *US Patent No. US5905613, 1999*.
10. Hinteregger H.F. and Müftü S., Contact tape recording with a flat-head contour. *IEEE Transactions on Magnetics* 1996, 32:5, 3476-3478.
11. Müftü, S. and Hinteregger H.F., The self-acting, subambient foil bearing in high speed, contact tape recording with a flat-head. *STLE Tribology Transactions* 1998, 41:1, 19-26.
12. Hinteregger H.F. and Müftü S., Flat-heads for contact tape recording: performance measurements at different wrap-angles, tape speed and tape stiffness. *Journal of Information Storage and Processing Systems* 1999, Vol. 2, pp. 75-82, 2000.
13. Müftü, S. and Kaiser, D.J., "Measurements and Theoretical Predictions of Head/Tape Spacing over a Flat-head," *Tribology International*, 2000, Vol. 33, pp. 415-430.

Appendix

In order to explain the displacement behavior of the mid-point of the tape presented in Figure 3 we investigate the strain energy stored in the tape as a result of the deformation described as case-1. The non-dimensional strain energy density stored in the tape over the head region is given by,

$$U = U_T + U_B = \frac{1}{2} \int_0^1 \left(\Delta^{-2} (w_{,xx}^{(2)})^2 + (w_{,x}^{(2)})^2 \right) dx \quad (\text{A1})$$

where $w^{(2)}$ is given by equation (9), U_T and U_B are the non-dimensional strain energy densities due to tension and bending resistance of the tape. In Figure 8 the U_T and U_B variations are plotted for $p = 0, 50$; $q = 3, 6, \text{ and } 9$; and $0 < \Delta \leq 10$. This figure shows that in the low Δ range the strain energy density in bending U_B is larger than the strain energy density in tension U_T . The contribution of the tension term U_T increases with increasing Δ ; indicating that in-plane resistance of the tape stores some of the external work. The U_T term peaks near the value of Δ_{cr} given in Figure 3. While the contribution of U_T increases, the strain energy stored in bending U_B decreases as shown in Figure 8. The magnitudes of the strain energy terms approach each other when $\Delta > \Delta_{cr}$. This corresponds to the flattening of the tape shown in Figure 4 when $\Delta > \Delta_{cr}$. It is concluded that the existence of the Δ_{cr} in Figure 3 is due to the peak of the tension stiffness of the tape.

Table Captions

- Table 1 Typical values of the physical parameters in a tape drive application, and the corresponding non-dimensional parameters. An unlikely, full evacuation of air over the head would cause $p^* = 101.3$ kPa

Figure Captions

- Figure 1. Figure showing a tape wrapped over a flat-head with wrap angle q , tension T subject to a negative uniformly distributed pressure p^* .
- Figure 2. Schematic description of tape deflection over a flat-head due to a uniform load acting downward over the head region.
- Figure 3 Mid-point displacement w_m of the tape, in case-1, as a function of the parameter Δ for $p = 0, 50$ and $q = 3, 6$ and 9 . Also shown is Δ_{cr} where the slope of the w_m versus Δ curve is zero.
- Figure 4 The effect of different Δ values, in case-1, on the displacement behavior of the tape; a) when $\Delta < \Delta_{cr}$ and b) when $\Delta > \Delta_{cr}$ for $p = 50$, $\theta = 6$ and $\Delta_{cr} = 3.84$.
- Figure 5 Displacement behavior of the tape over the flat-head at $\theta = 6$ for different loads p and a) for $\Delta = 10$ and b) for $\Delta = 50$.
- Figure 6 Variation of a) displacement bump length L and b) bump height $w|_{x=L_p}$ with external load p , in case-3, $p > p_{cr}^{(2)}$.
- Figure 7 The reaction forces F_0 and F_L for different Δ and q values for case-1, case2, and case-3.
- Figure 8 Strain energy density as a function of Δ , θ and a) $p = 0$, b) $p = 50$.

| Dimensional variables | | | |
|---------------------------------------|----------------------|----------------------|----------------------|
| Thickness, c [μm] | 5 | 15 | 5 |
| Poisson's ratio, ν | 0.3 | 0.3 | 0.3 |
| Elastic modulus, E [GPa] | 5 | 5 | 5 |
| Tape tension, T_{eff} [N/m] | 40 | 80 | 80 |
| Wrap angle, q^* [$^\circ$] | 1.5 | 3 | 5 |
| Head length, L_H [μm] | 200 | 300 | 500 |
| Pressure, p^* [Pa] | 5000 | 10000 | 25000 |
| Bending rigidity, D [Nm] | 5.7×10^{-8} | 1.6×10^{-6} | 5.7×10^{-8} |
| Bending length, b [μm] | 37.8 | 139 | 26.7 |
| Normalized variables | | | |
| Δ | 5.3 | 2.2 | 18.7 |
| q | 1 | 1 | 8.7 |
| p | 28 | 3.5 | 5460 |

Table 1 Typical values of the physical parameters in a tape drive application, and the corresponding non-dimensional parameters. An unlikely, full evacuation of air over the head would cause $p^* = 101.3$ kPa

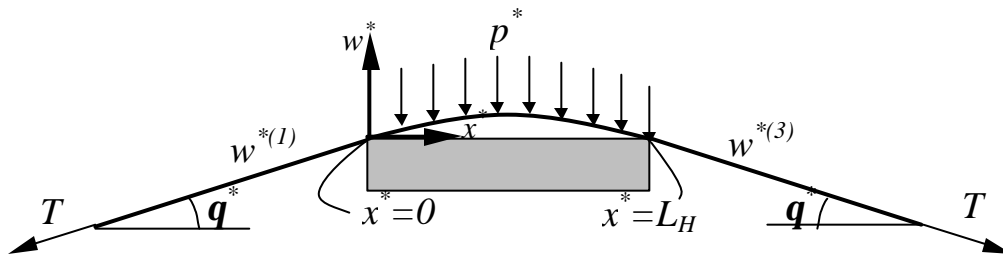


Figure 1. Figure showing a tape wrapped over a flat-head with wrap angle q , tension T subject to a negative uniformly distributed pressure p^* .

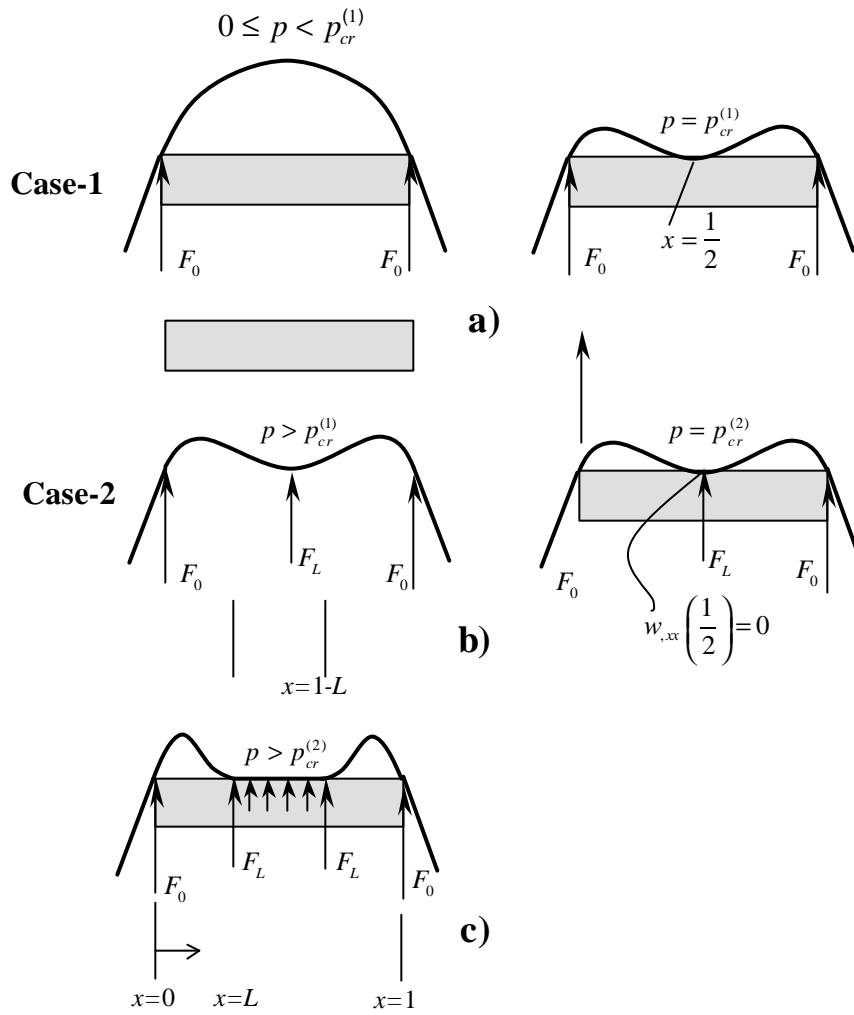


Figure 2. Schematic description of tape deflection over a flat-head due to a uniform load acting downward over the head region.

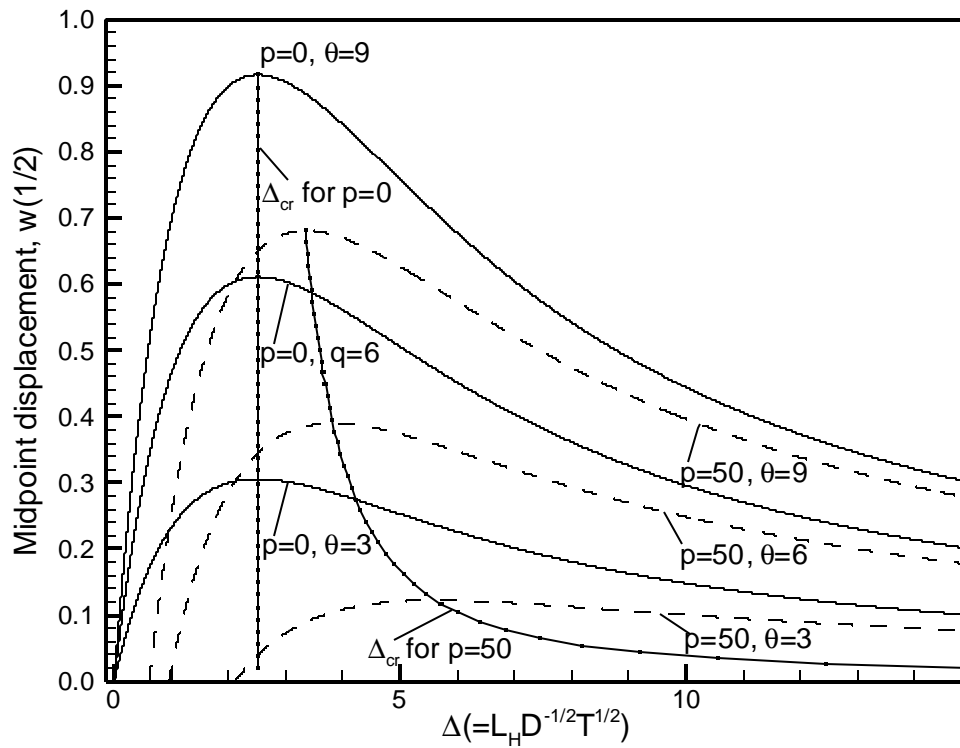


Figure 3 Mid-point displacement w_m of the tape, in case-1, as a function of the parameter Δ for $p = 0, 50$ and $q = 3, 6$ and 9 . Also shown is Δ_{cr} where the slope of the w_m versus Δ curve is zero.

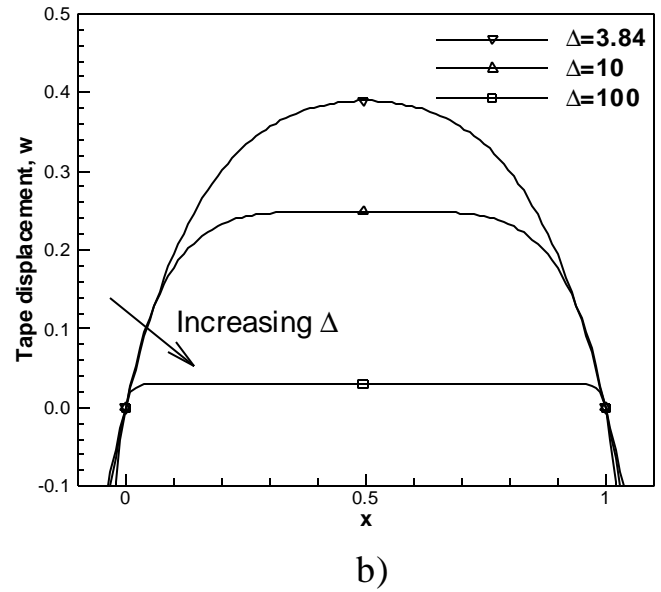
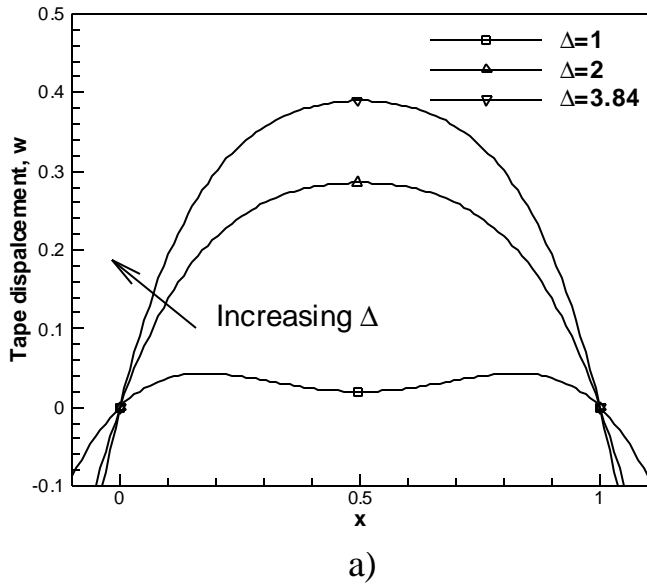
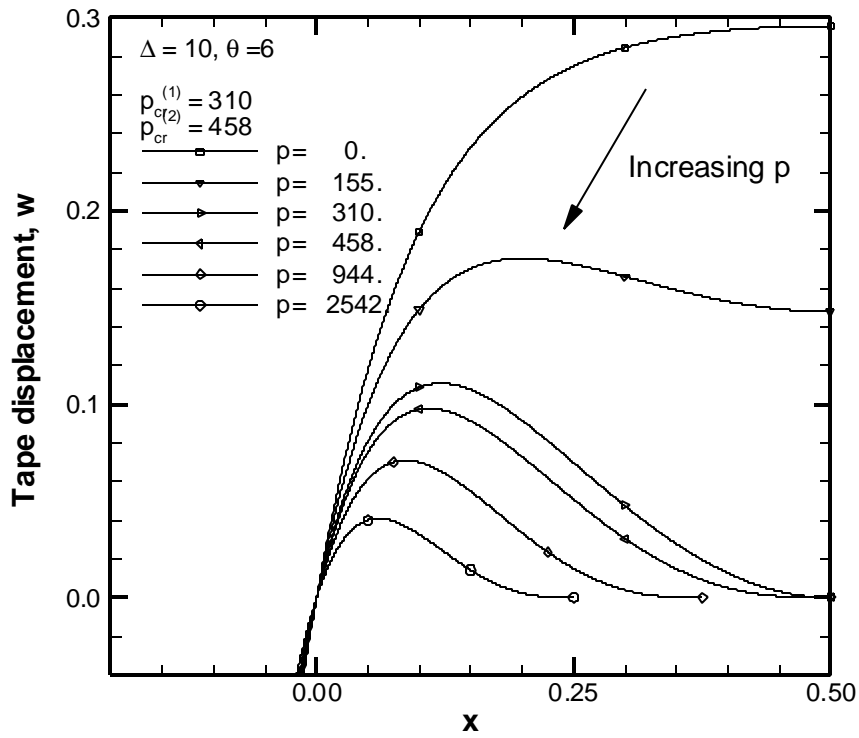
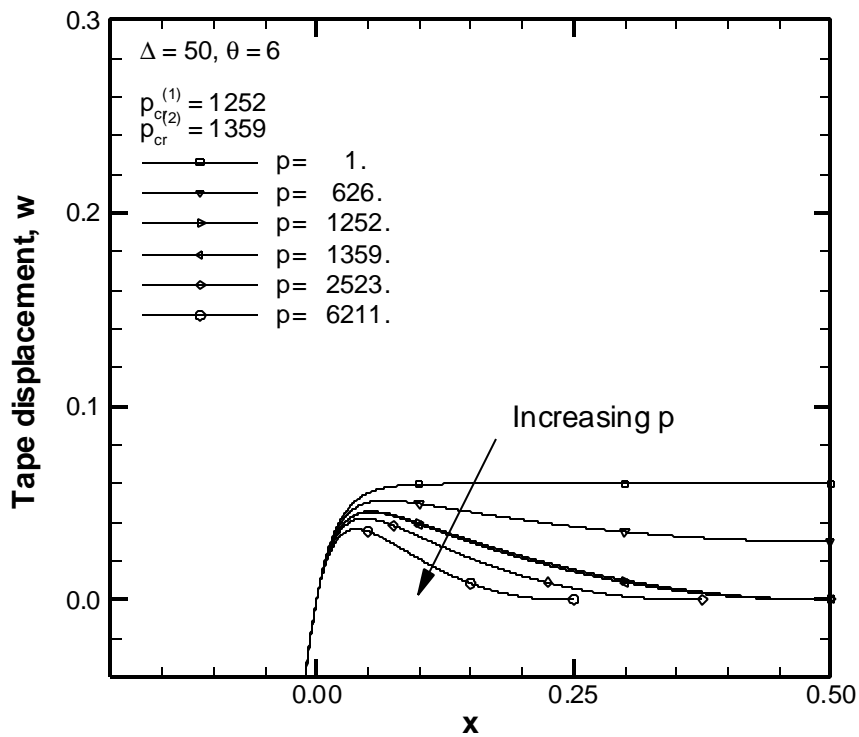


Figure 4 The effect of different Δ values, in case-1, on the displacement behavior of the tape; a) when $\Delta < \Delta_{cr}$ and b) when $\Delta > \Delta_{cr}$ for $p = 50$, $\theta = 6$ and $\Delta_{cr} = 3.84$.

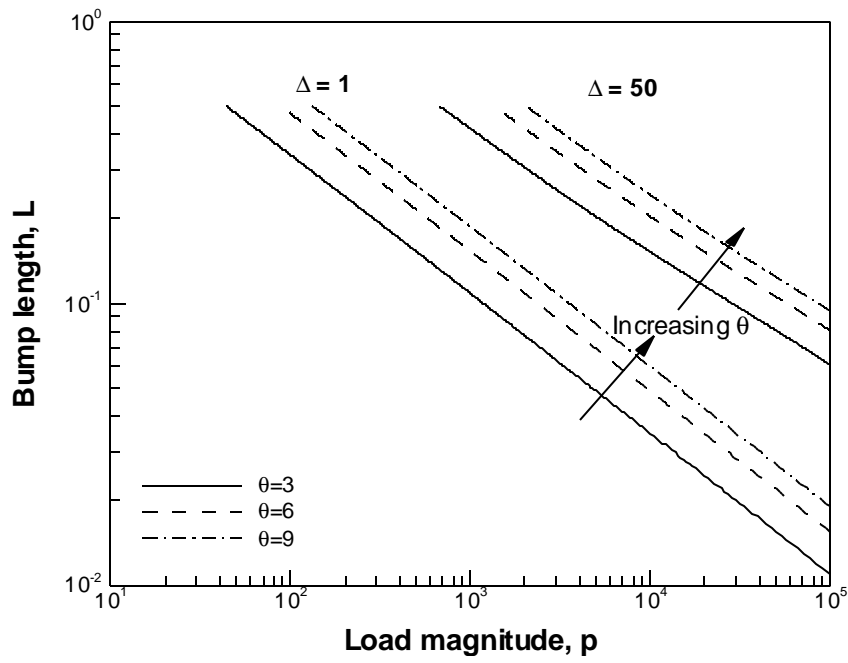


a)

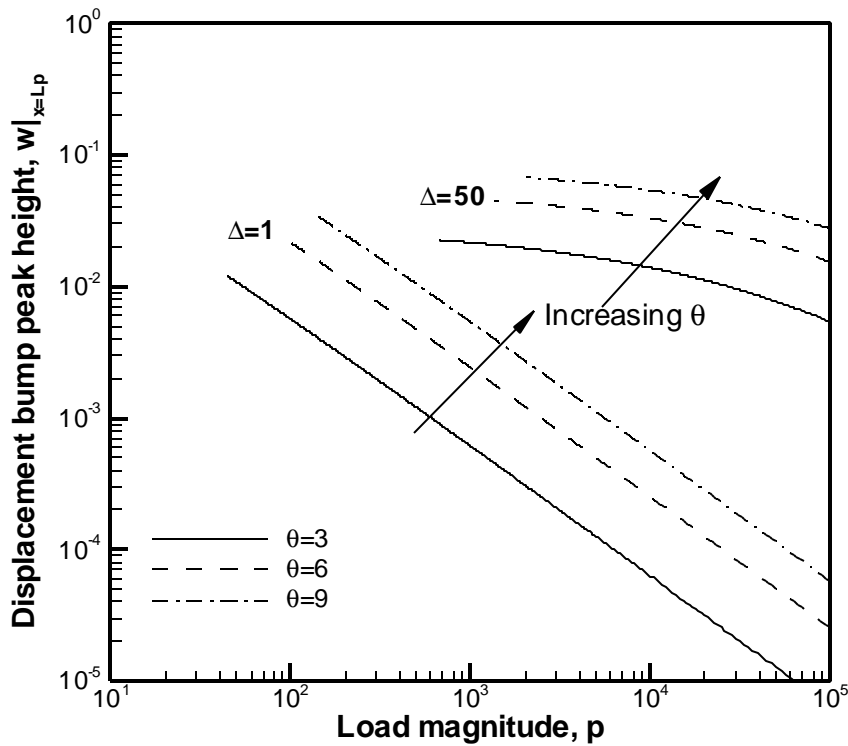


b)

Figure 5 Displacement behavior of the tape over the flat-head at $\theta = 6$ for different loads p and a) for $\Delta = 10$ and b) for $\Delta = 50$.

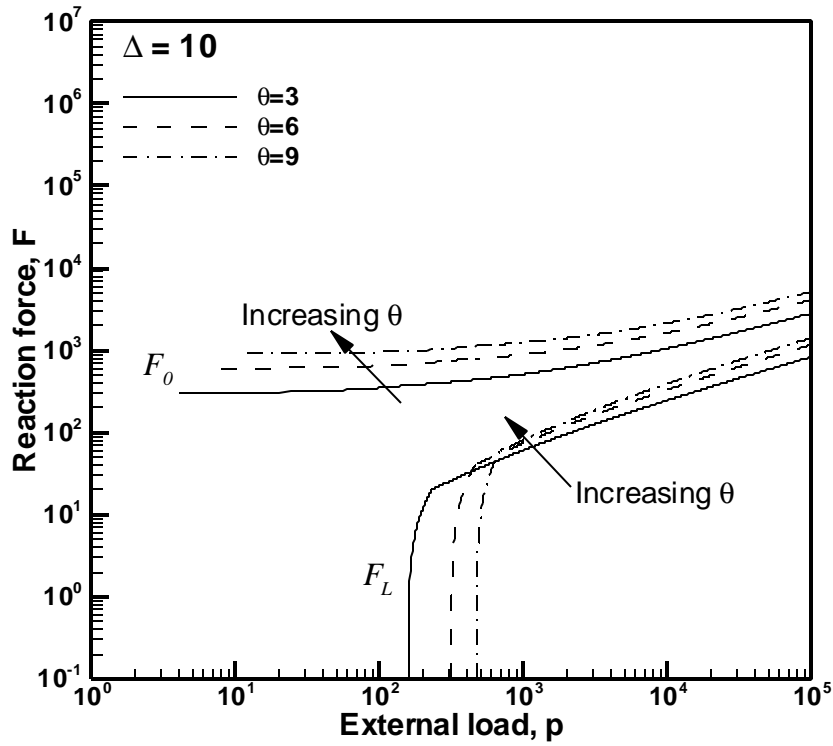


a)

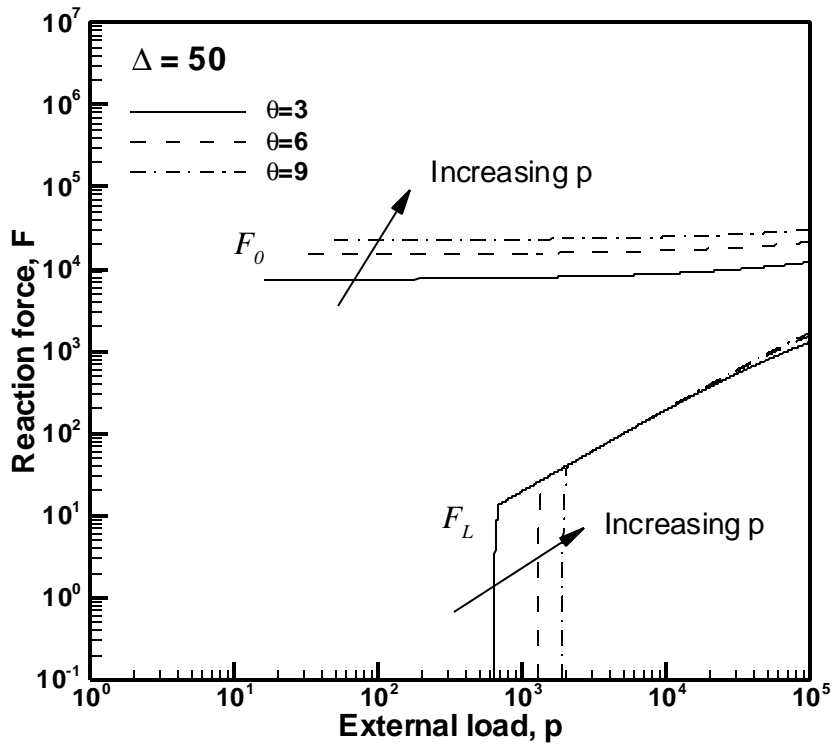


b)

Figure 6 Variation of a) displacement bump length L and b) bump height $w|_{x=L_p}$ with external load p , in case-3, $p > p_{cr}^{(2)}$.



a)



b)

Figure 7 The reaction forces F_0 and F_L for different Δ and q values for case-1, case2, and case-3.

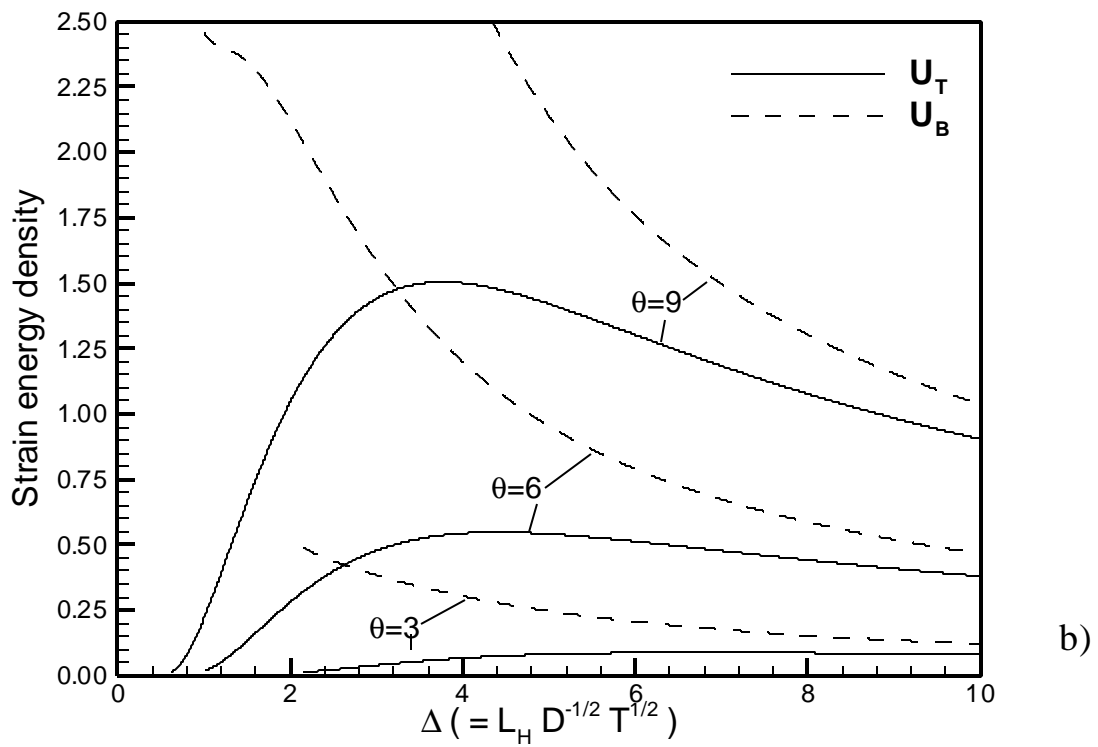
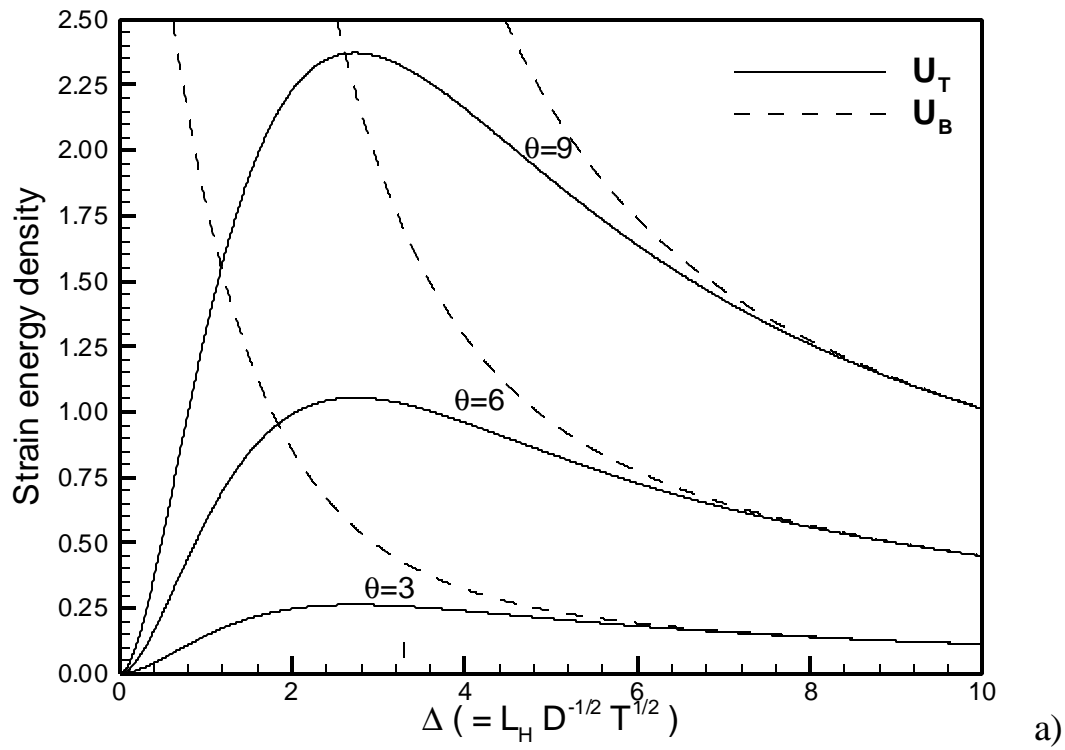


Figure 8 Strain energy densities U_T and U_B as a function of Δ , θ and a) $p = 0$, b) $p = 50$.